Integrated SPV-Battery BLDC Motor Drive Powered By Interleaved Boost Converter

Ronalisa Padhi
Dept. of Electrical Engineering
NIT,Rourkela
India
Ronalisa_padhi@nitrkl.ac.in

Kanungo Barada Mohanty
Dept. of Electrical Engineering
NIT,Rourkela
India
Kbmohanty@nitrkl.ac.in

Pavan Daramukala
Dept. of Electrical Engineering
NIT,Rourkela
India
519ee1001@nitrkl.ac.in

Bhanu Pratap Behera
Dept. of Electrical Engineering
NIT,Rourkela
India
beherab@nitrkl.ac.in

***Abstract*— Brushless Direct Current (BLDC) motors are one of the most rapidly expanding motor types. The modelling and control of a solar-powered BLDC motor drive are discussed in this paper. Solar photovoltaic (SPV) panels are linked to the three-phase Voltage Source Inverter (VSI) that powers the BLDC motor via a DC-DC Interleaved Boost converter (IBC). The efficiency of photovoltaic (PV) systems can be increased by using Maximum Power Point Tracking (MPPT) control algorithms at various dynamic conditions. PV systems have variable outputs that change with temperature and irradiance levels. When using a traditional boost converter, we experience a significant voltage ripple. When compared to a typical boost converter, the power electronics converter IBC aids in reducing ripple in power, input current, and output voltage. The analysis and design of two-stage IBCs are presented in this paper. Because of its great efficiency and dependability, enhanced performance, and low cost, BLDC motors are the ideal choice. The system under consideration, as well as the control mechanism, are formulated and simulated in the MATLAB-Simulink environment. With the inclusion of a battery management system, a constant and uninterrupted power supply is maintained despite shifting loads and irradiances. The battery's charging and discharging modes are also considered in this chapter.**

Keywords*— *Solar Photo Voltaic Module, Interleaved Boost converter (IBC), MPPT, Incremental Conductance MPPT(INC), Brushless DC Motor (BLDC).

I. INTRODUCTION

solar power generation is currently one of the most vital renewable energy sources due to its numerous benefits, including decreased carbon emissions and consistent availability. Numerous uses for photovoltaic arrays include battery charging, water pumping [1]-[4], grid connection, hybrid vehicles etc. A solar panel's optimum operating point is determined from its power-voltage (P-V) curve, which demonstrates that the PV delivers the greatest feasible power to the load at that point which varies with cell temperature, solar irradiation, and load. Solar energy's availability varies over time, so it's critical to take advantage of it while it's still available. There have been several ways to track maximum power point in the solar system [5]-[7]. It's critical to get the system to work at a specific point in order to get the most power out of it.

We employ Maximum power Point Tracking methods to draw power from a PV module. Any MPPT method's brain is a DC-DC converter that controls the source impedance, which fluctuates with atmospheric conditions, and changes the duty ratio to match the load impedance in order to maximise power transmission. In this paper, a PV system with a variety of environmental circumstances is taken into consideration. To handle these situations, MPPT techniques are needed, and the INC MPPT approach is utilised to extract the highest power possible regardless of the environment.

Boost converters outperform buck and buck-boost converters for solar applications [1]. Additionally, PV systems must meet requirements for high performance, affordability, and small size. However, the voltage stress across the switches in a conventional boost converter equals the output voltage, which reduces efficiency and causes switching loss. This issue can be solved by using an interleaved boost converter(IBC), which offers a large voltage gain with little losses and switch stress waived.

Interleaving, commonly known as multiphase, is a technique mostly employed for lowering filter size. Two converters are parallel-connected to a single load in interleaved converters. The disadvantage of the IBC is that during resonance, there is a very high voltage across the switch [8]-[10]. By using an ideal resonant inductor current value, this can be decreased. Values for the resonant inductor and capacitor have been determined according to the formula in order to attain the same results. This decreases the size of the passive components as well as the ripples in the input current. Finally, with fewer filter components, the capacitor current's peak-to-peak fluctuation also decreased. Input current ripple was also decreased.

Induction motors are now used in the majority of industrial applications because of improvements in power electronics and control methods. However, BLDC motors are gradually replacing induction motors because they are more efficient than induction motors, have greater speed-torque characteristics, and are smaller machines overall. In reality, a BLDC motor can be thought of as a DC motor that uses AC power [11]. We need to utilise an inverter to control BLDC motors, and the gate pulse of the inverter is typically produced from the hall voltage of the motor that is retrieved using Hall Effect sensors.

The BLDC motor's starting current is managed within the allowable range to ensure soft beginning. By correctly choosing the increment size in the INC-MPPT algorithm, the soft starting is accomplished. Along with that PI speed control of BLDC motor is done to control the speed in desired manner. Simulated results utilising the Sim-power system toolboxes of

979-8-3503-9976-9/23/$31.00 ©2023 IEEE

the MATLB/Simulink environment show the initial, dynamic, and steady state behaviour of the proposed system under the change in meteorological conditions.

II. THE SPECIFIED SYSTEM'S CONFIGURATION

The system consists of a solar photovoltaic array connected to Interleaved boost converter(IBC), followed by 3 phase VSI and BLDC motor. Here Incremental conductance MPPT (INC) is used to draw maximum power from the solar array by generating switching pulses for the IBC switches so that perfect switching sequence for the electronic commutation of BLDC motor using VSI is performed[5]. The encoder installed on the BLDC motor provides Hall Effect signals, which are logically transformed into 6 pulses for the 6 switches of the VSI. PI controllers are used to controlling the speed of BLDC motors. The planning and supervision of each phase of the configuration are depicted in the following sections.

A shared DC bus is produced by an SPV array using IBC and battery bank using a bidirectional buck-boost converter [1-2]. The MPPT of the SPV array is performed by the IBC using an INC method, and the charge controller for the battery is a buck-boost converter. This converter functions as boost when the battery is low, feeding the common DC bus with power from the battery. After the battery is charged and powered by the DC bus, the converter functions as a buck converter. An electrical commutation of a BLDC motor is carried out using a VSI. The shaft of a BLDC motor with three designed Hall Effect sensors that produce Hall outputs for commutation is connected to VSI for switching pulse. The block diagram of BLDC motor connected to solar photovoltaic module with battery storage system is sketched in Fig. 1.

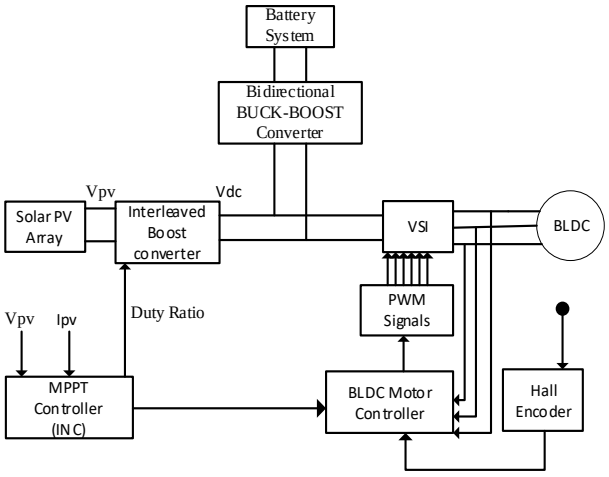

Fig.1. Scheme of BLDC Motor with SPV-Array

A. *Solar Photo Voltaic Array*

A PV module is made up of solar cells that are normally coupled in series or parallel to produce the proper output voltage and current. PV modules are interconnected in series and parallel connections to form a PV array. In fig. 2 single diode model of SPV is drawn. Solar irradiance and temperature have the greatest influence on the non-linearity in output characteristics of SPV, likely I-V and P-V curves. Since a PV module includes nonlinear properties, modelling a PV module is essential for precise design, operation, and the identification of the factors that lead to a decline in PV performance.

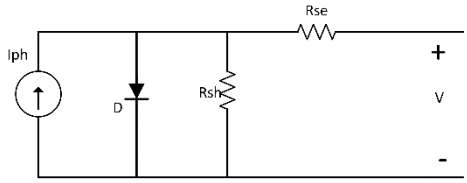

Fig. 2. Single Diode Model of SPV Module

The load current is derived as

$$I = I_{Ph} - I_0\left\{\exp\left(q\left(\frac{V+IR_s}{n.N_s.K.T}\right)\right)-1\right\}-\left(\frac{V+IR_s}{R_{sh}}\right) \quad (1)$$

Where Shunt current, diode current and reverse saturation of diode current can be approximated as

$$I_{sh} = \left(\frac{V+IR_s}{R_{sh}}\right) \quad (2)$$

$$I_0 = I_{rs}.\left(\frac{T}{T_n}\right)^3.\exp\left[\frac{q.E_{g0}\left(\frac{1}{T_n}-\frac{1}{T}\right)}{n.k}\right] \quad (3)$$

$$I_{rs} = \frac{I_{sc}}{\exp\left(\frac{q.Voc}{n.N_s.K.T}\right)-1} \quad (4)$$

It is possible to express Photovoltaic current as

$$I_{ph} = \left[I_{sc} + K_i\left(T-298\right)\right]\frac{G}{1000} \quad (5)$$

Where K is the Boltzmann' s constant and q is the charge of the electron having value as

$K= 1.38* 10^{-23}$

$q=1.6* 10^{-19}$ Coulomb

Table 1 contains the data sheet for the solar photovoltaic module.

TABLE 1. SPV Parameters

Parameters	Values	Parameters	Values
Open circuit condition voltage Vopen	64.2V	Short-circuit condition current	5.96A
Voltage at MPP, Vmp	54.7V	Cells in one module (Ncell)	96
Temperature coefficient	0.27269	Maximum Power	305.2W
Temperature coefficient Isc (%/deg.C)	0.061745	Light-generated current I_L	6.1A
Current at maximum power point Imp	5.58A	Diode saturation current I_0 (A)	6.3e-12
Shunt resistance Rsh	269.59 Ω	Diode ideality factor	0.95
Series resistance Rs	0.372Ω	Parallel modules (Npp)	4
Series modules (Nss)	2		

B. *Interleaved Boost Converter*

The interleaving method can reduce harmonics, reduce voltage and current ripples, and increase efficiency. Even if the diode (D) is blocking, the current in the inductor (I_L) starts to increase when the power devices switches are turned off, and the inductor begins loading. When switch (IGBT) is turned on, the converter's inductor begins discharging and transferring current to the load using the diode (D). The traditional Boost converter and interleaved Boost converter are drawn in fig. 3a and fig. 3b respectively. Two boost

converter units are interconnected in parallel[12], which are controlled using phase shifted switching technique (interleaved operation). Due to the parallel configuration, the duty cycle for each converter unit is equal to $(V_{out}-V_{in})/V_{out}$. However, there should be a phase shift of 180° between the first and second switching signals.

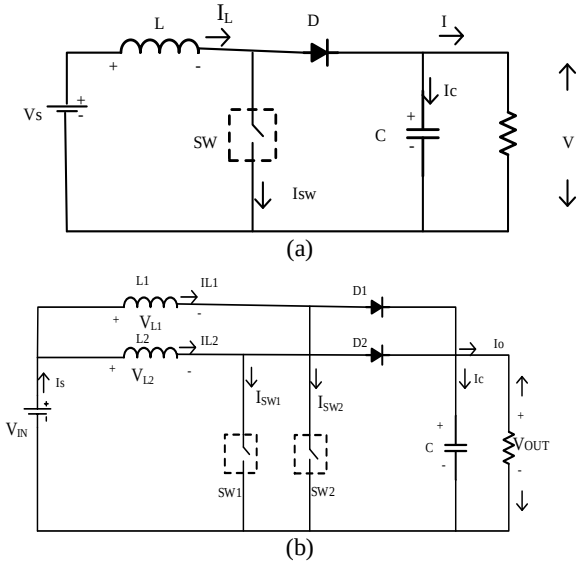

Fig.3 (a) Conventional Boost Converter, (b). Interleaved Boost Converter

Mode 1

S_{W1} is closed and S_{W2} is opened at time t_0. While L_2 continues to discharge, the inductor L_1's current starts to incr ease. IL_1 changes at a rate of $dIL_1/dt = V_{IN}/L$, whereas current in L_2 changes at a rate of $dIL_2/dt = (V_{IN} - V_{OUT})$

Mode 2

S_{W1} and $S_{W2\ are}$ opened at time t_1. Through the load, the inductors L_1 and L_2 are used to discharge. The change in IL_1 and IL_2 is expressed as $dIL_1/dt = dIL_2/dt = (V_{IN} - V_{OUT})/L$.

Mode 3

S_{W2} is closed at time t_2, however S_{W1} is still open. While L_1 continues to discharge, the current of the inductor L_2 begins to increase. While IL_1's rate of change is $dIL_1/dt = (V_{IN} - V_{OUT})/L$, IL_2's rate of change is $dIL_2/dt = V_{IN}/L$.

Mode 4

S_{W1} is still open at time t_3, but S_{W2} is now open. The load causes the inductors L_1 and L_2 to discharge. IL_1 and IL_2 change at a rate of $dIL_1/dt = dIL_2/dt = (V_{IN} - V_{OUT})/L$.

The two stages interleaved Boost converter has the same duty ratio as a traditional Boost converter.

$$V_{OUT} = \frac{V_{IN}}{1-D} \tag{6}$$

Where D is the duty ratio that varies from 0 to 1, the input power is determined from the formula

$$I_{IN} = \frac{P_{IN}}{V_{IN}} \tag{7}$$

The following form is used to calculate the capacitance (C) and inductance (L) design parameters for a two-stage interleaved boost converter.

$$C = \frac{(V_s.D.f_{sw})}{R.\Delta V_o} \tag{8}$$

$$L = \frac{V_s.D}{\Delta I_L.f_{sw}} \tag{9}$$

TABLE 2. Interleaved Boost Parameters

Parameters	Value	Unit
Switching Frequency(f_{SW})	5000	kHz
Capacitor (C)	3000	µF
Inductor (L_1 , L_2)	25	mH

C. MPPT algorithm

The maximum power output from the SPV is derived using incremental conductance (INC) algorithm [4]. This technique uses the instantaneous conductance (I/V) and the incremental conductance (dI/dV) to track the peak power. The installed PV array is always utilised to its full potential using an MPPT approach. An INC is the most widely used of the numerous developed approaches because of its high tracking performance in dynamic conditions. The duty ratio was selected as an input parameter for the suggested system. According to the power slope, the duty ratio is perturbed at a constant perturbation size and rate. The relationship between the two parameters conductance and incremental conductance can be used to determine where the PV module's operational point is located on the P-V curve. Based on the relationship between these two values, it is possible to pinpoint the location of the PV module's desired value in the P-V curve, as demonstrated by equations (10), which shows that the PV module operates at the MPP, and (11) and (12), which demonstrate that the PV system operates on the L.H.S and R.H.S of the, respectively, in the P-V curve.

$$\frac{dI}{dV} = -\frac{I}{V} \tag{10}$$

$$\frac{dI}{dV} > -\frac{I}{V} \tag{11}$$

$$\frac{dI}{dV} < -\frac{I}{V} \tag{12}$$

The P-V graph at MPP is assumed to have a slope of zero, which is the basis for the equations described above, i.e.

$$\frac{dP}{dV} = 0 \tag{13}$$

The following equation can be created by rewriting equation (13).

$$I + V\frac{dI}{dV} = 0 \tag{14}$$

Fig. 4 depicts the flow chart of INC algorithm following which maximum power from SPV can be drawn.

D. Dynamic Modelling of BLDC Motor

Similar to three phase synchronous machines, BLDC motor modelling can be constructed. Certain dynamic properties are unique since the rotor is attached with a permanent magnet. The magnet determines the flux linkage from the rotor. As a result, this type of motors frequently experiences magnetic flux linkage saturation. The BLDC motor is fed by a three-phase voltage source, similar to other common three phase motors. The phase voltage of BLDC motor can be explained as in eq.(15).

$$\begin{bmatrix} u_A \\ u_B \\ u_C \end{bmatrix} = \begin{bmatrix} R & 0 & 0 \\ 0 & R & 0 \\ 0 & 0 & R \end{bmatrix} \begin{bmatrix} i_A \\ i_B \\ i_C \end{bmatrix} + \begin{bmatrix} L-M & 0 & 0 \\ 0 & L-M & 0 \\ 0 & 0 & L-M \end{bmatrix} \frac{d}{dt} \begin{bmatrix} i_A \\ i_B \\ i_C \end{bmatrix} + \begin{bmatrix} e_A \\ e_B \\ e_C \end{bmatrix} \quad (15)$$

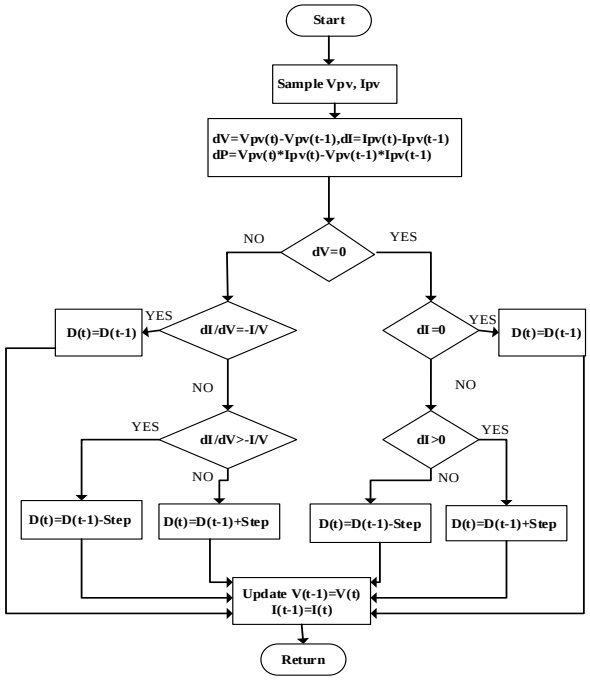

Fig.4. Flow Chart of INC Algorithm

$$e_A = 2NS\omega B_m f_A(\theta) = \omega \psi_m f_A(\theta) \quad (16)$$

The power delivered to the rotor, known as electromagnetic power, equals the product of the three phases' current and back-EMF. That is

$$P_e = e_A i_A + e_B i_B + e_C i_C \quad (17)$$

The electromagnetic power is converted into kinetic energy by ignoring mechanical losses and stray losses.

$$\text{So} \quad P_e = T_e \Omega \quad (18)$$

Where T_e is Electromagnetic torque and Ω is the Angular velocity of rotation. Moreover, the torque equation can also be represented as

$$T_e = p\left[\psi_m f_A(\theta) i_A + \psi_m f_B(\theta) i_B + \psi_m f_C(\theta) i_C\right] \quad (19)$$

Where p is the pole pairs count.

The complete mathematical modelling of the electromechanical system can be written using the motion equation as mentioned in (20).

$$T_e - T_L = j\frac{d\Omega}{dt} + B_v \Omega \quad (20)$$

Where T_L represents the load torque; J- Rotor moment of inertia; and B_v - viscous friction coefficient.

By adjusting the DC bus voltage of VSI at the specified DC voltage of the BLDC motor, the motor speed is controlled[11]. By controlling the DC bus voltage and subsequently the operating speed, a bi-directional power flow control makes it possible to deliver the entire amount of power needed to the load at maximum capacity. The phase current sensors are removed in the recommended BLDC motor drive, resulting in a straightforward and affordable control.

TABLE 3. BLDC Motor Parameters

No. of Poles	4	ϕ linkage constant	0.175 V.sec
No. of Phases	3	Equivalent Ls	0.0085 Henry
Y/Δ	Star	Moment of Inertia	0.0008 kg-m^2
Vdc	306 V	Damping constant	0.001 N-m/rad
Resistance/Ph	2.8750 Ω	Rated Power output	1.8 Hp
Speed Range	±1200 rpm	Rated Max Torque	11 N-m

E..Storage Battery Charging Management

A buck-boost converter is utilized to transfer power between the DC bus and storage battery in both the directions using the control logic as depicted in Fig. 5. The DC bus voltage controls the mode of operation. A current regulator regulates the battery's charging and discharging current. The voltage and current are controlled by a proportional-integral (PI) controller. The appropriate duty ratio is provided by the current regulator, and it is then transformed into a PWM switching pulse for the buck-boost converter. One of the two operating modes for the buck-boost bidirectional converter is used at once.

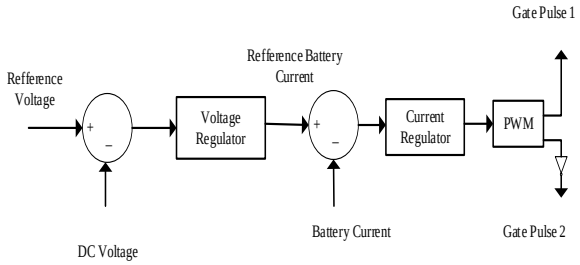

Fig.5. Block diagram OF Bidirectional charge control of Battery

During the night, when solar energy is absent and when it is at its lowest, there is a decline in the DC bus voltage. The converter operates as boost so that power flows from battery to DC bus, discharging the battery and maintaining the voltage level at its predetermined value. In contrast, the DC bus voltage increases when the SPV power is available, but no power is needed for the load. By running the converter as buck and regulating the power transform from DC bus to battery, controller is able to maintain the voltage level at the predetermined value and recharge the battery. In contrast, when an SPV array generates enough power to maintain the load at its maximum capacity, the battery is rendered inoperable. There is no charging or discharging of the battery.

III. OUTCOMES AND DISCUSSION

Using MATLAB-Simulink toolboxes, the suggested system's performance under various operating situations is analyzed. A 1200 rpm @ 300V; 11Nm BLDC motor is driven by a hybrid generating unit of a 2.7 kW peak SPV array of 164 Volt output integrated with 400 Ah lead-acid battery. The system's exact design is best utilized for water irrigation in agriculture sector, industry supply and other domestic & industrial usages. Depending on how much sunlight is available, it is possible to operate the BLDC motor load entirely with the SPV array, alone with the battery, or both

with the SPV and battery. The following study clarifies how the system operate. This study evaluates the system's dynamic reaction under insufficient solar irradiation i.e., Performance while transitioning from supplying a load through SPV array to a combination of SPV array and a battery

Two scenarios of irradiance and temperature are taken for simulation in Fig. 6 i.e of 1000 w/m^2 & 45^0 C (Scenario-A, good atmospheric Condition i.e, from 0-3 sec.) and 300 w/m^2 & 15^0 C (Scenario-B, worst atmospheric condition i.e, from 3-6 sec., resulting in output power reduction to nearly one third than scenario-A). When low radiation is observed, the battery is automatically put into effect. In both the scenarios, the motor performance remains unaffected under different atmospheric condition. This case scenarios are illustrated in Fig. 6. Three different load torque with three different reference speed {(i)11NM torque 1100 rpm speed, (ii) 10NM torque 900rpm speed, (iii) 9NM torque with 700rpm speed} has been taken under observation for better study of drive dynamics of BLDC motor under scenario-A and B,as depicted in Fig. 6.

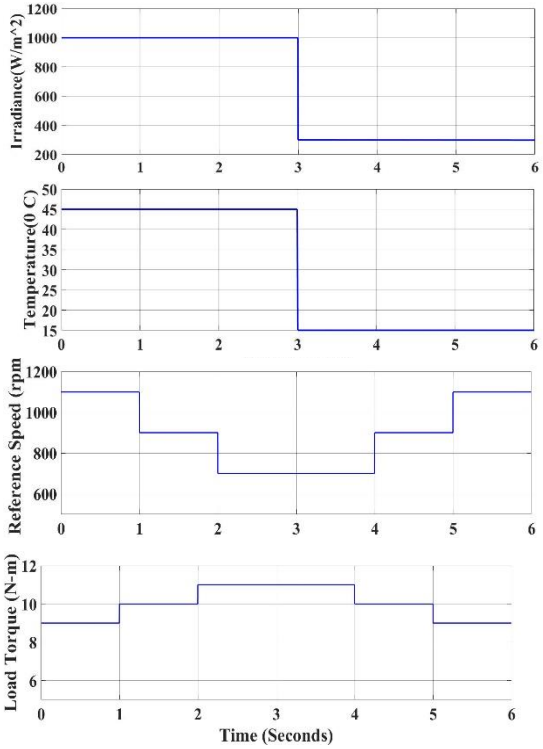

Fig. 6. (Irradiance, Temperature, Speed reference and load torque under consideration.)

The SPV array feeds the load until the solar irradiation in between 500 W/m^2-1000 W/m^2 which is enough to run the load of 1400W at maximum availability (0 to 3 Sec). The battery is therefore getting charged at irradiance above 500 W/m2 and stays in an idle condition at 500 W/m2. The battery is not drained of current and is kept at 50% i.e., at initial charging state. The SPV array's output power has been cut in half, so sharing the load demand is necessary to keep the load running at peak capacity. When the irradiance is below 500 W/m2, (3 to 6 Sec) utilising the Buck-Boost converter the battery gets discharged by the control technique of bidirectional power flow, and the rest power is pulled from

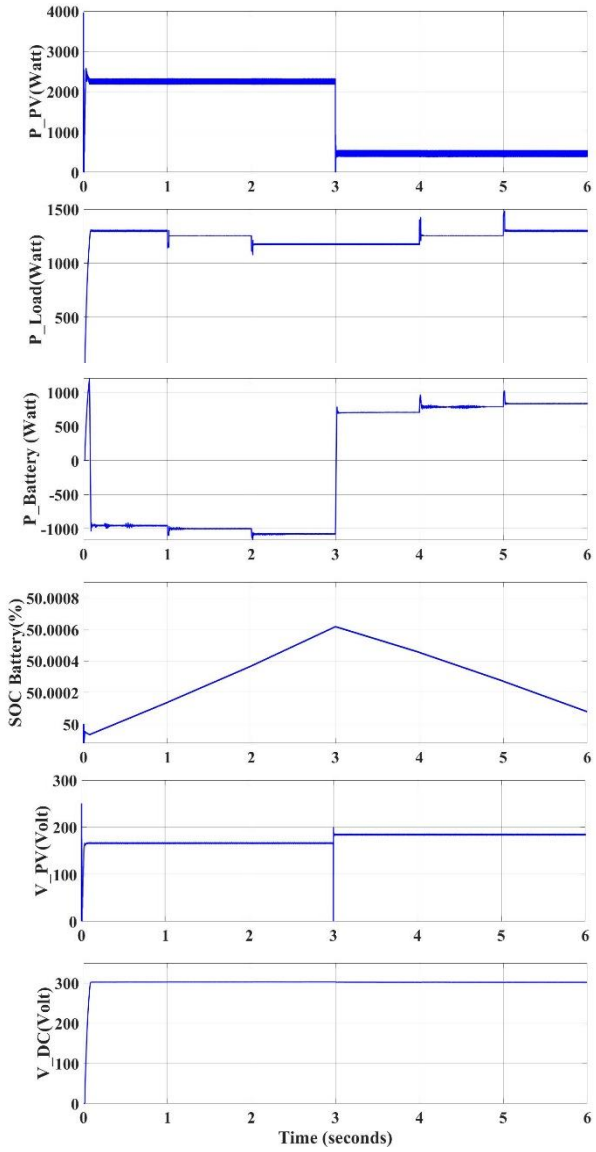

Fig. 7. (P_PV, P_Load, P_Battery, SOC, V_{PV} and V_{DC} of the proposed system.)

the battery. Consequently, the battery and SPV array both supply power to the load. This scenario illustrated in Fig.7.

Here, While keeping the Vdc at 306 V, the buck-boost converter functions as a boost converter to supply power to the DC bus in Scenario B and as a buck converter in Scenario-A. The DC link voltage output of the Boost module is maintained by the voltage output of the PV array and Battery connected to the DC bus through proper feedback control circuits and which control the gate drive circuits of IBC and Bidirectional Buck/Boost converter. The Power input (P_PV), Power output (P_Load), Power flow through battery (P_ Battery) and state of charge (SOC%) of the battery, the Input voltage; $V_{\_PV}$ and DC link Voltage V_{DC} are depicted in Fig. 7.

The torque developed is in accordance with the load torque and is represented in Fig. 8 (a) and Fig. 8 (b) shows the desired speed achieved by the motor through BLDC Motor PI-DTC control circuit in compared with reference speed taken in Fig. 6.

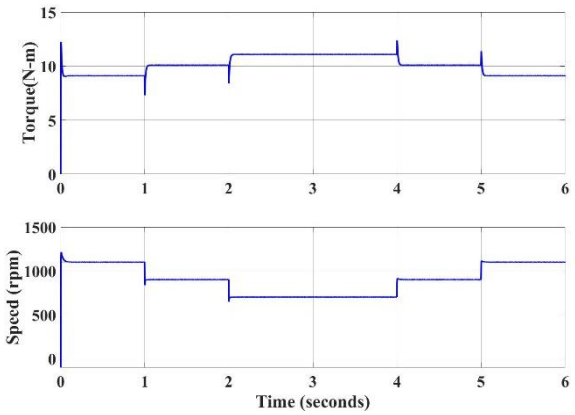

Fig. 8. (Torque developed, and Speed of BLDC Motor).

By using the two stage IBC the ripple in the input current of the system reduces to almost 50% which is shown in Fig. 9. Hence performance improved.

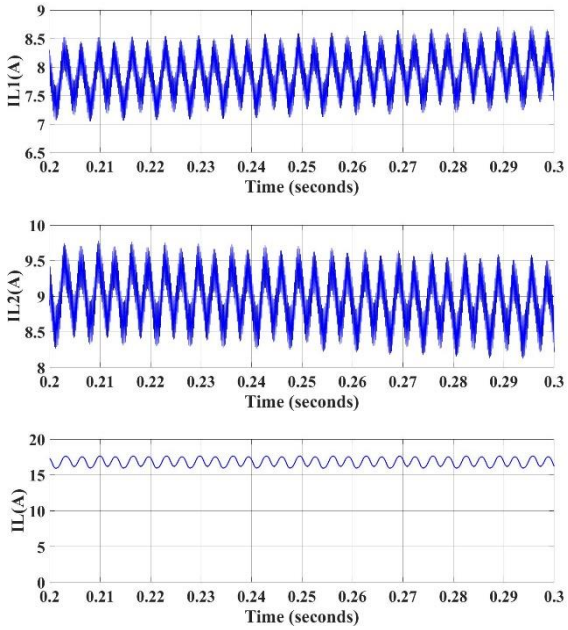

Fig. 9 (Inductor 1 current IL_1, Inductor 2 current IL_2 and I/P current IL)

IV. Conclusion

This proposed model is designed and run in Matlab/Simulink environment and we see that the model in both atmospheric conditions considered (Scenario-A & B) operates well irrespective of loading on motor with the desired speed taken under consideration. The bidirectional buck-boost converter connected battery helps the system run efficiently with no drop in DC bus voltage as well as supply power to motor load in bad weather condition. The two stage IBC converter aid less ripple input current so as improved the performance of system over single boost converter fed BLDC motor drive.

IV. References

[1] R. Kumar and B. Singh, "Solar PV-battery based hybrid water pumping system using BLDC motor drive,"2016 IEEE 1st International Conference on Power Electronics, Intelligent Control and Energy Systems (ICPEICES), 2016, pp. 1-6

[2] S. G. Sigarchian, A. Malmquist & T. Fransson, "Modelling and Control Strategy of a Hybrid PV/Wind/Engine/Battery system to Provide Electricity and Drinkable Water for Remote" Applications. *Energy Procedia, 57,* 1401-1410 , (2014).

[3] S. S. Dash, T. Pradhan, S. Bastia and D. P. Bagarty, "An Interleaved Soft-Switching Boost Converter Based Isolated Solar PV with Integrated Battery System," 2020 IEEE International Symposium on Sustainable Energy, Signal Processing and Cyber Security (iSSSC), 2020, pp. 1-5

[4] R. Kumar and B. Singh, "Single Stage Solar PV Fed Brushless DC Motor Driven Water Pump," *IEEE Journal of Emerging and Selected Topics in Power Electronics*, vol. 5, no. 3, pp. 1377-1385, Sept. 2017.

[5] K. B. Sahay and A. Yadav, "Implementation of MPPT Technique in PV Array for a Varying Load by Modeling and Simulation," *International Electrical Engineering Congress (iEECON)*, 2018, pp. 1-4

[6] K. Jain, M. Gupta and A. Kumar Bohre, "Implementation and Comparative Analysis of P&O and INC MPPT Method for PV System," *8th IEEE India International Conference on Power Electronics (IICPE*), 2018, pp. 1-6.

[7] M. A. Elgendy; D. J. Atkinson and B. Zahawi; "Experimental investigation of the incremental conductance maximum power point tracking algorithm at high perturbation rates," lET Renewable Power Generation; vol. 10; no. 2; pp. 133-139; Feb. 2016.

[8] D. Y. Jung, Y. H. Ji, S. H. Park, Y. C. Jung and C. Y. Won, "Interleaved Soft-Switching Boost Converter for Photovoltaic Power-Generation System," *IEEE Transactions on Power Electronics*, vol. 26, no. 4, pp. 1137-1145, April 2011

[9] N. Rana, M. Kumar, A. Ghosh and S. Banerjee, "A Novel Interleaved Tri-State Boost Converter With Lower Ripple and Improved Dynamic Response," *in IEEE Transactions on Industrial Electronics*, vol. 65, no. 7, pp. 5456-5465, July 2018

[10] X. Xu, W. Liu and A. Q. Huang, "Two-Phase Interleaved Critical Mode PFC Boost Converter With Closed Loop Interleaving Strategy," *IEEE Transactions on Power Electronics*, vol. 24, no. 12, pp. 3003-3013, Dec. 2009

[11] R. Shanmugasundram, K. M. Zakariah and N. Yadaiah, "Implementation and Performance Analysis of Digital Controllers for Brushless DC Motor Drives," *IEEE/ASME Transactions on Mechatronics*, vol. 19, no. 1, pp. 213-224, Feb. 2014.

[12] M. Malik and A. Ali, "A two cascaded boost converter with high voltage gain module," International Journal of Computer and Electrical Engineering (IJCEE), vol. 9, pp. 476–483, 09 2017.

[13] B. Singh and R. Kumar; "Solar photovoltaic array fed water pump driven by brushless DC motor using Landsman converter," lET Renewable Power Generation; vol. 10; no. 4; pp. 474-484; April 2016.